

THE CONTRIBUTION OF ARTIFICIAL INTELLIGENCE TO AERIAL PHOTOINTERPRETATION OF ARCHAEOLOGICAL SITES: A COMPARISON BETWEEN TRADITIONAL AND MACHINE LEARNING METHODS

1. INTRODUCTION

It is well known that aerial photographs are a useful working tool for specialists in various scientific fields (town planners, landscape architects, geographers, geologists, agronomists); in fact, they are vital for archaeologists specializing in the study of historical topography and ancient cities. The advantage provided by aerial photography is demonstrated by the possibility of detecting buried archaeological features through the “marks” showing up on the photograms, so to define with precision the geometric outline of buildings and burials or the course of underground road paths. Among the different types of tracks (damp-marks, crop-marks, soil-sites, shadow-sites) this research focuses mainly on crop-marks as they are characterized by a deep colour contrast. In fact, archaeological structures interact with the vegetation’s rooting apparatus deeply influencing its growth so that it can be either reduced or enhanced. In aerial photographs, this difference clearly appears in the chromatic contrast.

For example, in case of graves dug in the ground or defensive ditches, the vegetation will be taller and thicker, resulting in a dark green colour; on the contrary, plants over masonry structures or roads will be lower and thinner resulting in light green or yellow. Summing up the accurate methodology applied to the study of aerial photographs and to the restitution of archaeological traces (PICCARRETA 1987; ALVISI 1989; PICCARRETA, CERAUDDO 2000; GUAITOLI 2003; MUSSON, PALMER, CAMPANA 2005), once the photointerpretation activity has been completed, the specialist draws the archaeological evidence on a topographical map in order to locate it on the ground ahead of stratigraphic excavations or of more ordinary activities of protection, land management and development. This operation, which in view of its purposes requires a high degree of precision, can essentially be carried out in two ways: with the technical instrumentation used to produce topographical maps (analytical or digital photorestituturs), or using a professional software for georeferencing and orthorectifying the images and then CAD digitizing of the marks.

Only the first case involves real “photorestitution”. It requires an operator highly qualified in cartographic techniques and an archaeologist expert in aerial photointerpretation (archaeologists-cartographers trained

in both skills being unfortunately rare); the degree of precision achieved is centimetric or sub-centimetric depending on the scale at which the zenithal frames are taken. In the second case, instead, it is more correct to use the word “vectorisation” or “digitalisation” of the marks. This is a less accurate mapping method, however sub-metric. Regardless of the method employed and specialisation of the archaeologist, both for the photointerpretation phase of the traces and for the mapping on paper, many days of work are necessary to complete the research.

Starting from the experience gained in the ARCHEO 3.0 project “Integration of key enabling technologies for the efficiency of preventive archaeological excavations”¹, where automatic systems were applied for the automatic or semi-automatic tracing of the contours of archaeological layers detected in excavations through the use of photographic images (CACCIARI, POCOBELLI, SIANO 2017; CACCIARI *et al.* 2018), here we aim at verifying the feasibility of artificial intelligence systems for marks recognition in aerial imagery and at assessing its practical use in order to speed up the graphic recording time (CACCIARI, POCOBELLI *in press*).

The use of artificial intelligence is currently explored by other researchers, although in different contexts. In this respect, the advanced stage achieved by the experimentation of artificial intelligence systems on World War II historical aerial photographs in the field of civil security, for the recognition of traces from exploded and unexploded ordnance must be mentioned (OZDEMIR, REMONDINO 2019; SHEPHERD *et al.* 2019).

In this article we present a summary of the procedure adopted and the results obtained. Issues deriving from image geo-referencing will be dealt with in a further work.

2. MATERIALS AND METHODS

2.1 *Data-set and acquisition methods*

The present research availed itself of aerial images of Vulci, one of the most important cities of ancient Etruria from which, according to epigraphic and archaeological documents, Servius Tullius, the legendary sixth king of Rome, came from. In my PhD in Ancient Topography I carried out a research on Vulci with the prevalent use of aerial photographs, in order to map the archaeological marks visible in the urban area and the surrounding necropolis

¹ Two Institutes of the Italian National Research Council – the Istituto di Fisica Applicata “Nello Carrara” (IFAC) and the Istituto per la Conservazione e Valorizzazione dei Beni Culturali (ICVBC), now Istituto di Scienze del Patrimonio Culturale (ISPC) – have been actively involved in the project ARCHEO 3.0, co-funded by the Tuscany Region (POR-CReO/FESR 2014-2020). The wide-ranging competences of the CNR Institutes has allowed to exploit ICT solutions in order to develop automatic methods of acquisition and graphic rendering of archaeological layers.

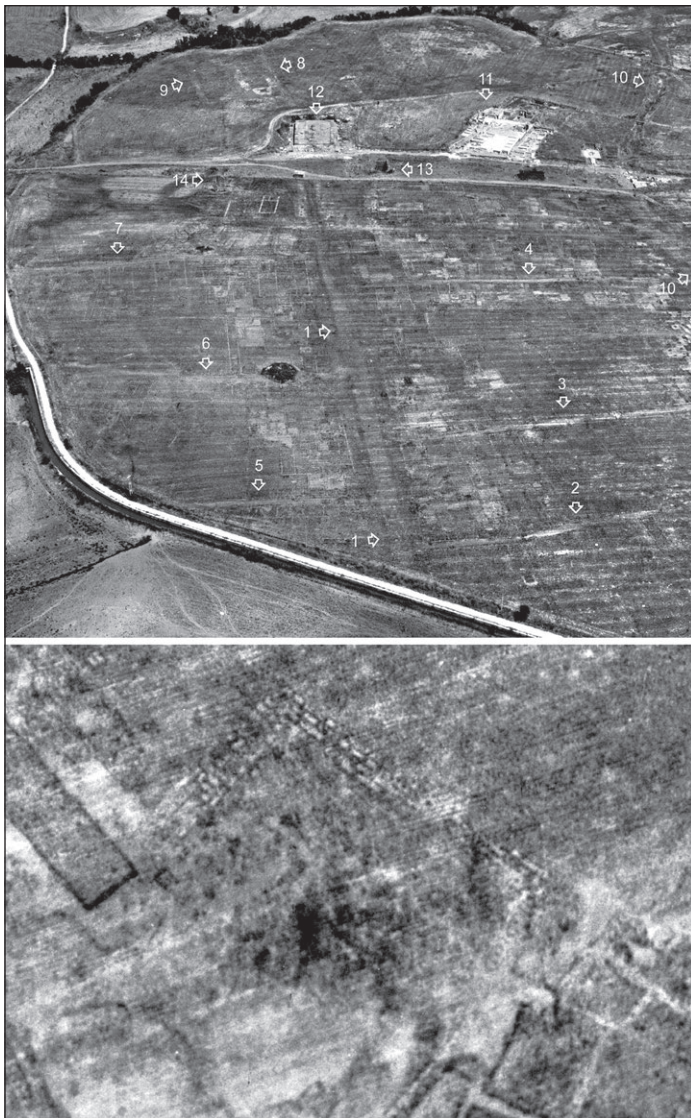


Fig. 1 – Vulci. Top: the 1975 perspective photograph showing the marks of the city's urban plan as seen from the S. Clearly visible are the main NS road (1) and the secondary roads that delimit the blocks (2-9). Around the large dark area of the "Foro Occidentale" are the "Tempio Grande" (12), the "Edificio Absidato" (13), the "Edificio in Laterizio" (14), on the right, the "Domus del Criptoportico" (11) and the so-called "Cardine Massimo" (10). Bottom: detail of the 1975 perspective photo with traces of the Etruscan temple in *opus quadratum* at the so-called "Foro Orientale" (POCOBELLI 2011).



Fig. 2 – Vulci. The 1975 low-altitude photo with marks visible in the so-called “Foro Occidentale” area (POCOBELLI 2004).

(POCOBELLI 2006). Using the traditional methods of archaeological photo-interpretation and cartographic restitution my research achieved significant results. For example, the ancient town plan of the city was reconstructed, with the road network (Fig. 1) and the perimeter of the Western Forum in front of the famous “Tempio Grande” (Fig. 2), apparently overlooked by a small theatre (POCOBELLI 2003, 150-151; 2004, 131-133).

Moreover, in the city’s NE area, at the foot of the acropolis, marks of an Etruscan temple have been identified (Fig. 1, bottom), located along the eastern side of a further area with a public function, the so-called “Foro Orientale”, previously unknown (POCOBELLI 2003, 151-154; 2004, 133-136; 2011, 120). Excavations carried out after this discovery has confirmed the existence of a sacred building in *opus quadratum* (MORETTI SGUBINI, RICCIARDI 2011, 79-80). The traces found in the necropolis area are also interesting (POCOBELLI 2007, 170-183). For instance, to the N of the ancient city, in the Poggio Mengarelli area, aerial imagery has clearly shown the crop-marks determined by features excavated in the tufaceous bank (Figs. 3, 7). The rectangular marks are simple pit graves used at the end of the 8th century BC, while the architecturally more complex chamber tombs (i.e. the T-shape to be seen in the photographs), with a long ramp (*dromos*) and a rectangular *atrium* leading to the funerary hypogea, were built by aristocratic families from the 7th BC c. onwards (POCOBELLI 2003, 154-156; 2007, 173-174). In

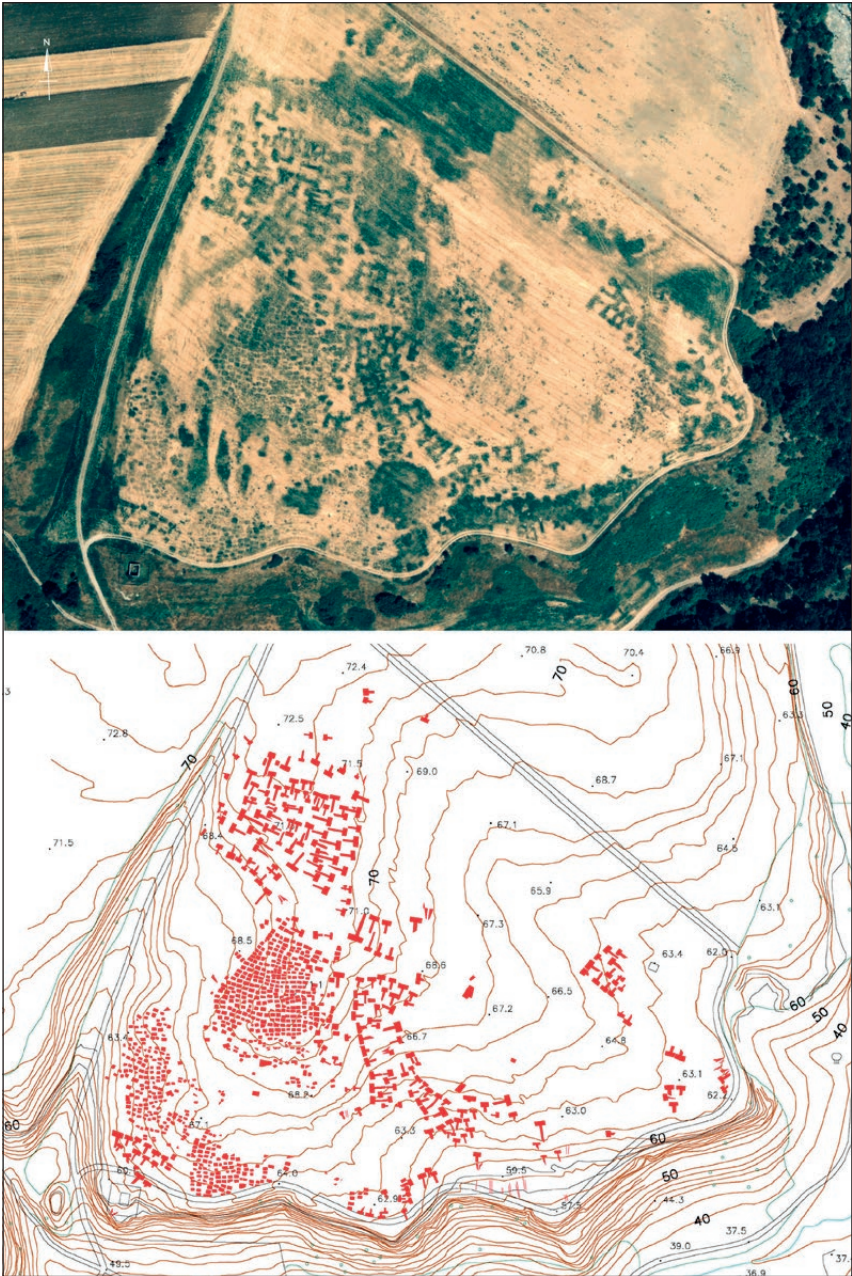


Fig. 3 – Vulci, Poggio Mengarelli. The 1997 aerial photograph and the photogrammetric restitution of the marks of the pit and chamber tombs (POCOBELLI 2007).

whole, this research allowed the mapping of more than 1600 pit graves and 1275 chamber graves.

The analytical data from this previous study are here used as a comparative basis in order to evaluate qualitatively and quantitatively the results obtained. The tests were carried out on colour and B/W aerial photographs of both the urban area and the surrounding necropolis, by selecting images with a high number of marks and with different characteristics (damp-marks, crop-marks, soil-sites, shadow-sites), in order to verify the system's response to different types of archaeological anomalies. Each single image was digitized in uncompressed format (*.tiff) with a flatbed scanner, in colour mode (24 bit depth), at different resolutions (150, 300, 600 dpi) in order to assess the impact on the detection ability of the individual traces.

In detail, the tests were carried out on some zenithal images of the urban area, where the marks of roads delimiting the residential blocks are easily identifiable (SIAT 1986 and CGRA 1997 flights), and on other perspective images taken at lower altitudes (Lisandrelli 1975 flight) with a higher mark definition (POCOBELLI 2004, 130-140) (Fig. 2). In the case of the necropolises, instead, images from the Poggio Mengarelli area were chosen, where some 1997 aerial zenithal images and oblique photographs taken at lower altitudes clearly show the planimetric development of the pit tombs, identified by their rectangular crop-marks, and of the chamber tombs, easily recognisable by the T-shape of the *dromos* with vestibule, all of which were photo-restituted (POCOBELLI 2007, 172-174) (Fig. 3). The images used in this research, with the exception of the perspective photographs of the necropolis taken by the author, belong to the collection of ICCD-Aerofototeca Nazionale.

G.F.P.

2.2 Image enhancement

The images considered in this work are affected by background intensity variations. For this reason, some areas of the captured scene result brighter than others. This has suggested the need of a specific filtering operation in order to improve the image reading before any further operation. Images undesirably affected by background intensity variations can be corrected by flat-field techniques. In general, this is accomplished with the following operation performed to each pixel in the image:

$$I_c = (I_o - o) \times g \quad (1)$$

where I_c and I_o represent the intensity of the corrected and original pixel, respectively, o and g represent an offset and gain values that are different for each pixel. A calibration procedure is required in order to estimate both the offset and gain values. This is accomplished computing pixel data from the

dark and the flat image. The dark image is captured by covering the sensor, the flat by using a uniform object covering the whole field of view. Several dark and flat images are then acquired and the corresponding average considered for flat field calculation. The intensity of a pixel in the dark image represents the offset coefficient. The intensity of the corrected pixel is defined as the value to be corrected for the flat image:

$$A_f - D_d = (f - d) \times g \quad (2)$$

where A_f and D_d represent the average field and dark images respectively, and f and d the pixel intensity of the flat and dark images respectively, and g the gain. Once the gain values have been computed from inverting eq. (2), a specific correction for each pixel of the image can be performed. This general procedure allows achieving an accurate representation of the background intensity as well as removing sensor noise.

Unfortunately, it is not possible to perform neither dark nor field images, and it is not also possible to create multiple images. For these reasons, in this work the flat field cannot be directly measured but only estimated. The flat field estimation has been performed by fitting the surface with a 2D polynomial mathematical model on the image intensity. A sampled grid of pixels has been chosen in order to fit the model. The higher is the grid size (or the polynomial model), the higher is the accuracy achieved.

Prior to applying colour clustering, all the original images have been considered as RGB coloured. The flat field estimation has been performed individually on the three colour planes and the results combined back into an RGB image to be subtracted to the original image. An example of the improvement obtained with flat field correction is shown in Fig. 4. The original image (Fig. 4a) shows a dark zone in the upper right part, the flat field estimated considering a grid size of 32×32 pixels and a third degree polynomial model shows a non-uniform background (Fig. 4b). In the final image (Fig. 4c), after flat field correction the background appears more uniform and the shadows in the upper right part of the images seem to be reduced.

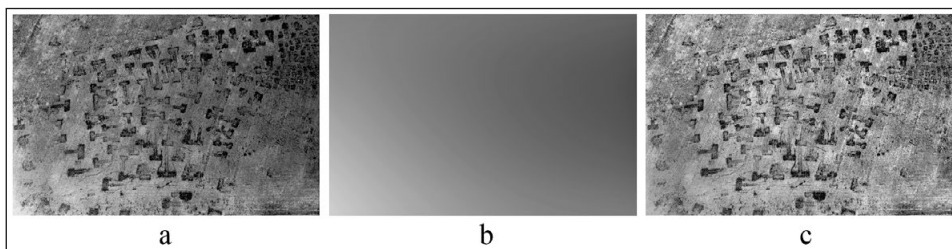


Fig. 4 – a) original image; b) estimated flat field; c) flat field corrected image.

2.3 Machine Learning unsupervised algorithm for colour clustering

The range of applications involving Machine Learning (ML) techniques spans virtually all sectors: from product recommendations (PORTUGAL, ALENCAR, COWAN 2018) to medical diagnoses (BAKATOR, RADOSAV 2018; XU, XUE, ZHANG 2019) to financial analysis (GU, KELLY, XIU 2020).

It is interesting to observe that this also involves disciplines that, for a long time, have been considered distant from this technology. It is then not surprising that archaeology has also benefited from ML. In particular, what sounds appealing in the archaeological community is the capability of unsupervised ML techniques to identify groups in a data set according to specific features (named as clusters). This task is commonly referred to as unsupervised learning. Since in the archaeological context, the features to be identified are often partial or completely unknown, the unsupervised clustering may provide the earliest grouping of the available datasets involving minimal human intervention and a limited initial input data set. This appears even more intriguing in all the cases in which archaeology works with images. In fact, from a preliminary division of an image provided by unsupervised clustering, unexpected things may appear. This could help the archaeologist in the identification of similar features that otherwise could not be easily observable with naked eye.

Among the numerous unsupervised ML algorithms for clustering, in this work we have considered k-means clustering (REILLY, RAHTZ 1992). The widespread diffusion of k-means algorithm is essentially due to its easy implementation and robustness. K-means image clustering is used with unlabelled data (i.e. data without defined categories). The aim is to partition the sample data sets (image pixels) into a pre-specified number of clusters (k) based on some kind of similarity in the data within the k clusters.

The algorithm we have implemented for this work starts with the number of clusters (k) and the type of colour coordinates (RGB, HSL, etc.), both established *a priori* by a human operator. At this stage, the human can also change some image parameters such as “brightness”, “contrast”, and “gamma”, in order to enhance details in the coloured image. Moreover, the human operator can also apply a low pass filtering operator in order to smooth the image. The resulting image is fed to the algorithm for colour clustering. K pixels in the image are picked in a random fashion. These pixels represent the first guess of the clusters centers (barycenters). Then a distance measurement (e.g. Euclidean distance) is calculated between each data point and the first guess of the barycenters. This calculation allows assigning each point to the closer cluster by reducing the in-cluster distance between all pixels. The cluster barycenters are then recalculated and new assignment made. The iteration is repeated until no further change occurs in the barycenters. A schematic representation is depicted in Fig. 5.

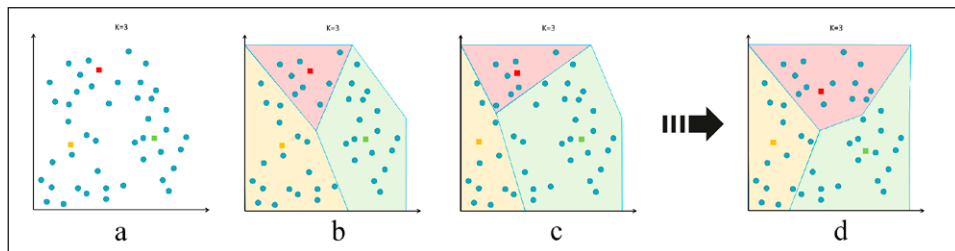


Fig. 5 – K means clustering: a) original dataset including the first guess of the barycenters; b) first grouping of the original dataset in three clusters; c) and d) update of the barycenters locations and new clusters development; d) end of the algorithm with the identification of final clusters and corresponding barycenters.

At the end the algorithm has assigned each pixel in the original image to a specific cluster. As output, the original image is separated into k images, in which all the non-zero pixels belong to a specific cluster. An 8-bit number is then associated to all the non-zero pixels in one of the k images. This assignment is then repeated with different 8 bit numbers for the remaining k images. The resulting k images are combined into a composite image that is finally used with standard edge detection technique to highlight the clusters contours.

3. RESULTS AND DISCUSSION

Although in the proposed algorithm the human intervention could be considered limited, it could affect the results in terms of marks identification. As described above, the number of clusters and the type of colour coordinates are both established *a priori* by the human operator. In this work, the entire colour clustering analysis has been performed considering only two clusters. This heuristic choice has been motivated by the interest in separating the tomb contours from the background, as if there were only two elements (clusters) to be identified.

On the contrary, the colour coordinates choice deserves a thorough discussion, and cannot be defined with heuristic motivations. As preliminary tests, some images have been colour clustered making use of RGB, HIS, HSV, CieLab and CieXYZ colour coordinates. The reader unfamiliar with the colour coordinates if interested could benefit from the available literature on this topic (MEYER, GREENBERG 1980; IBRAHEEM *et al.* 2012; KAHU, RAUT, BHURCHANDI 2019). As an example in Fig. 6 is reported the contour obtained with clustering using different colour coordinates. The images in Fig. 6 evidence that some colour space can bring out certain details better than others. Although in the presented example the CieXYZ coordinates seem to offer the

best results, it should not lead us to claim that it is of general validity. What could be confidently stated is that any case should be preliminarily discussed in order to determine the best results.

Since in this work we are just interested in comparing the human results with the machine ones, we have focused the analysis only on RGB coordinates, exploring instead the effect of image resolution as well as the difference among coloured and black and white images.

I.C.

The results obtained through ML algorithms, in the case of aerial photographs of the urban area, have evidenced low definition in terms of contour recognition. This can be explained considering that the large amount of information and the variability of the traces generate a background noise that does not allow a correct distinction of the shapes. This outcome is found both in images taken by airplane (high altitude flights) and proximity photographs (drone or low altitude flights), regardless of the image resolution. This is mainly due to the intrinsic characteristics of the linear tracks (mostly structures and roads), which are not uniform in colour over their entire extension and are therefore difficult for the algorithm to recognise. In this area, what is intelligible to the human eye, at the current state of experimentation, is not fully answered by the system's processing.

On the 1997 aerial photographs, the ML system was able to detect the outline of the marks in more detail than in the urban area, although it showed severe limitations in tracing individual graves due to the reciprocal proximity of the burials and the advanced growth of the vegetation (Fig. 7). However, areas with the presence of burials are well defined. Better results were obtained with low altitude photographs of the necropolis. The test also demonstrated the impact of image resolution on the final result. At a low resolution (150 dpi) the system succeeded in defining the macro-areas affected by the burials and roughly the contours of 15 graves (Fig. 8a); at 300 dpi, although the background noise is still evident, the details of the traces appear improved and 27 graves can be recognised (Fig. 8b). At medium-high resolution (600 dpi) the shapes of 34 chamber tombs can be seen; the presence of more burials helps in further delimiting the area (Fig. 8c).

Of even higher interest is the result obtained in this area with panchromatic images. In order to compare data, the same photographs were printed in bichromatic mode (see e.g. the image in Fig. 8) and scanned with the same parameters (Fig. 9). The differences are evident: already at 150 dpi the algorithm is able to distinguish, with good approximation, the geometry of most (52) of the recognizable chamber tombs (Fig. 9a) and at 300 dpi the tombs outlined are 68. At 600 dpi the definition of the contours is optimal (Fig. 9c), with 96 well-defined chamber tombs which, although results are in part

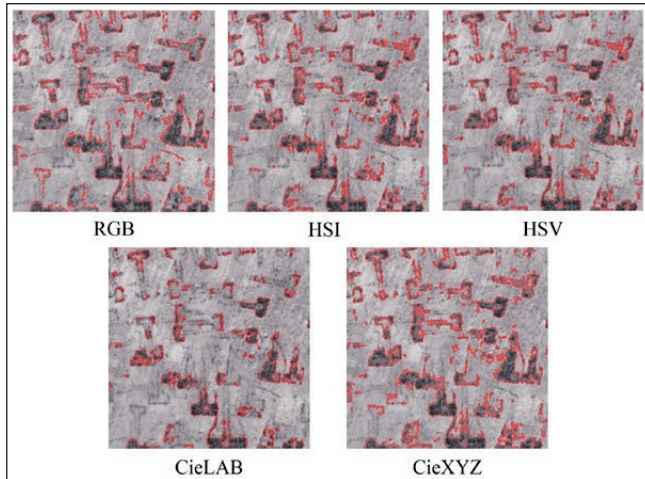


Fig. 6 – Contours obtained after colour clustering with different colour coordinates.

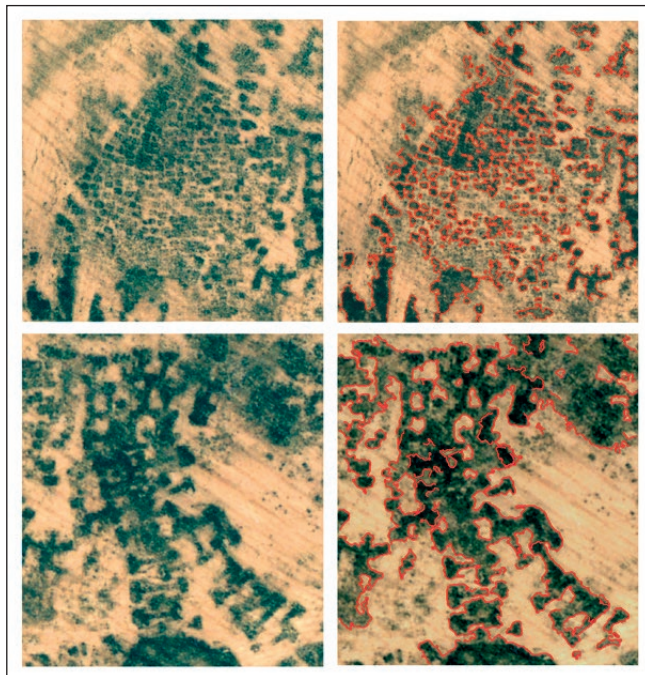


Fig. 7 – Vulci, Poggio Mengarelli. Aerial original image: details of crop-marks of pit tombs and chamber tombs (left); with ML outlines (right).

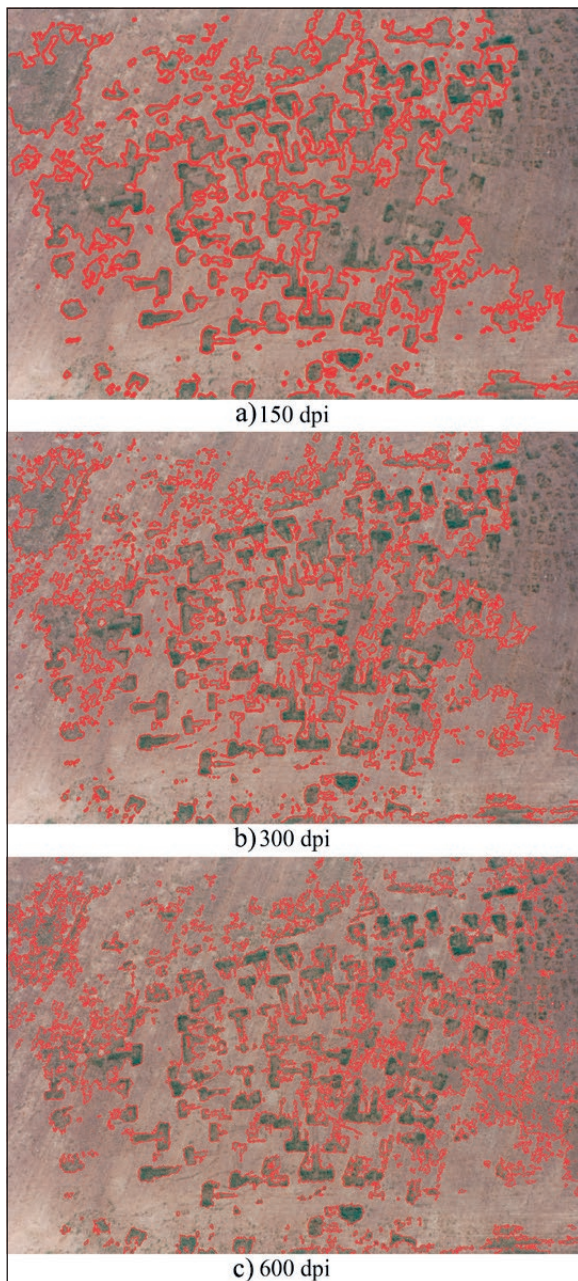


Fig. 8 – Contours obtained performing RGB colour clustering on coloured images of different resolution.

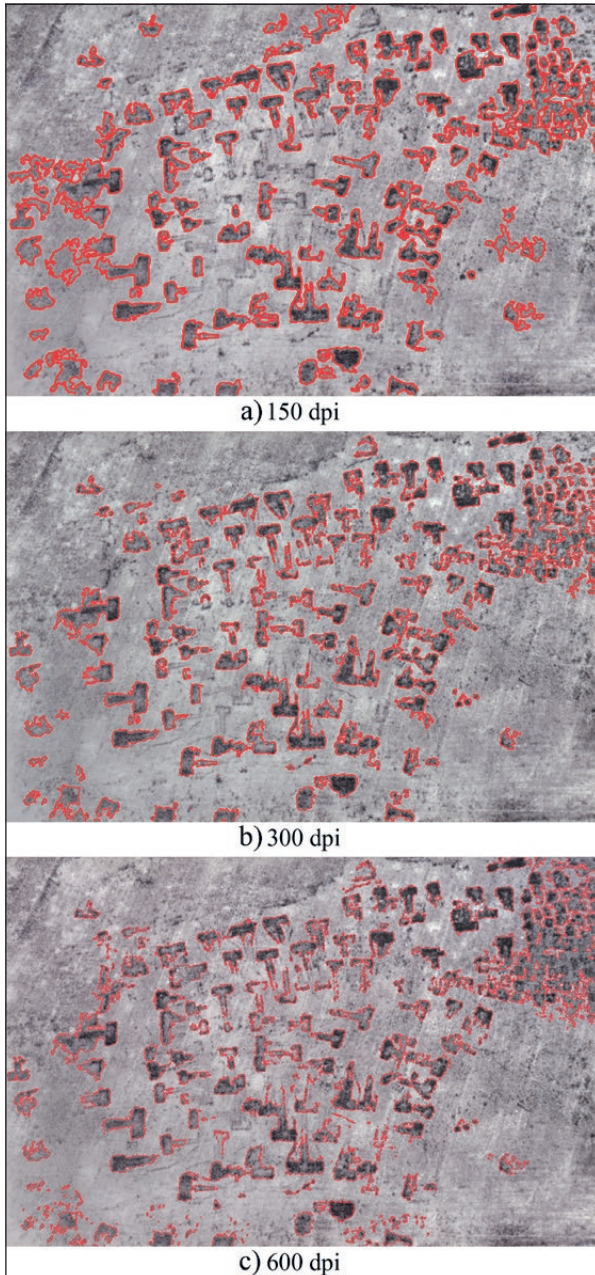


Fig. 9 – Contours obtained performing RGB colour clustering on B/W images of different resolution.

indecisive, especially in the definition of the *dromoi*, correspond to a percentage of 81.3 compared to what was mapped with the traditional method.

G.F.P.

4. CONCLUSIONS AND FUTURE PERSPECTIVES

Research has demonstrated that ML developed in the framework of the ARCHEO 3.0 project for the identification of archaeological strata under excavation, with appropriate calibrations and corrections can also be applied to aerial photographs for the recognition of archaeological traces, with interesting development prospects.

An in-depth analysis, however, shows that the response of the system is highly variable. The first consideration concerns the characteristics of the tracks. As expected, the system works well with crop-marks. In the area of the necropolis, where the graves show a well-defined contrast with the surrounding area, ML image processing produces individual traces with good results.

Conversely, where the vegetation colour is rather uniform or the marks are not clearly defined, the system is unable to distinguish individual elements but defines a contour area. In other cases, as in the urban area, where the human eye recognizes the regular forms of structures and road, the proposed automatic system is not able to detect marks.

Best results are achieved with low altitude photographs in the necropolis area, where the algorithm correctly distinguishes and highlights the profiles of the individual chamber tombs, with little loss of information.

The difference with the 1997 aerial photos depends on the different degree of detail in the image. In addition to the altitude at which the images were taken, the type and condition of the vegetation influence the possibility of reading the marks: in the field sown with alfalfa, the low altitude photos were taken in the first days of June, with vegetation in its initial state of growth, while the others were taken at the end of July. However, in aerial images, the areas with higher vegetation, where the photointerpreter distinguishes numerous tracks, are well defined.

The difference in system processing between colour and B/W photographs is also very interesting. Fig. 10 clearly shows the graphical result of the marks within the two types of photos: the wider range of chromatic shades leads to greater noise, resulting in confusion in the drawing of shapes. Instead, the smaller amount of grey tones allows for greater detail and a better ability of the algorithm to precisely define the contour of the track.

Comparison with the traditional mapping method suggests that the ML system needs further improvements. With regard to the amount of information useful for the graphic detection of graves, for example, tests on the colour image at 600 dpi (Fig. 8c) indicate that the algorithm defines 34 chamber graves,

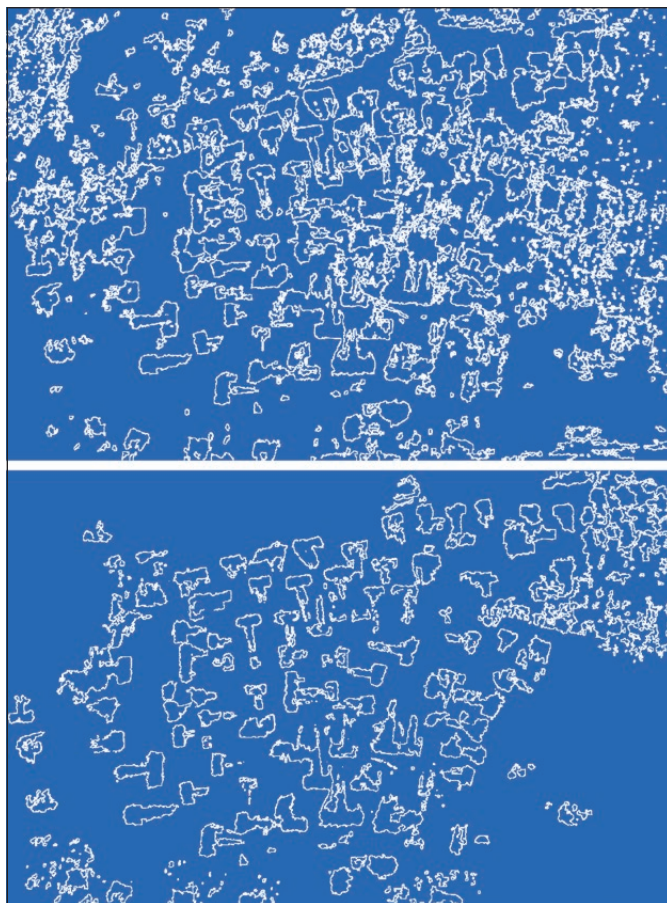


Fig. 10 – Outlines obtained with 600 dpi photo (see Figs. 8 and 9): colour (top) and B/W (bottom).

28.8% of the burials mapped by the traditional method (118), while in the B/W photo the marks – drawn with good shape definition (Fig. 9c) – are 96 (81.3%).

The cartographic comparison is also good: contours processed with ML show great realism and have a substantial correspondence with the marks mapped with the traditional restitution method. The small differences that can be found are due to the orthorectification of oblique images, which is not necessary for zenithal photographs. The error found is only a few tens of centimetres, comparable to the deformations that occur with CAD vectorisation of the tracks. Human intervention, however, is still necessary to integrate what is not detected by the algorithm.

The failure to identify traces recognisable by the human eye – one of the limitations shown by the system – could be overcome by processing the same image several times with different parameters and filters, to create different layers of reading that, overlapping, can integrate the information gaps.

Image definition is perhaps another element to be considered in order to obtain better results, although increasing resolution up to 1200 dpi and the colour depth to 48 bit (now 600 dpi at 24 bit colour) makes the data to be processed heavier.

On the basis of the current experience, future elaborations will be carried out considering also the preliminary transformation of images from colour to B/W and also comparing the use of further algorithms and possibly exploring neural networks.

For the overall evaluation of the achieved results, the amount of time necessary to map the tracks is crucial. With the traditional method and the expensive technical equipment for cartographic restitution, certainly more precise and complete, it takes two or three days of work, while the proposed ML system and a standard computer require only a few tens of seconds.

However, despite the limitations highlighted in this experimentation, it is plausible that, with suitable improvements, ML systems will be valuable tools for significantly accelerating the time spent in graphical restitution. This in turn will help the archaeologist not specialised in cartographic restitution to map buried archaeological remains with decimetric approximation, in order to plan excavations and promote their enhancement and protection.

I.C., G.F.P.

ILARIA CACCIARI

Istituto di Fisica Applicata “Nello Carrara” – CNR
i.cacciari@ifac.cnr.it

GIORGIO F. POCOBELLI

Istituto di Scienze del Patrimonio Culturale – CNR
giorgiofranco.pocobelli@cnr.it

REFERENCES

- ALVISI G. 1989, *La fotografia aerea nell'indagine archeologica*, Roma, La Nuova Italia Scientifica.
- BAKATOR M., RADOSAV D. 2018, *Deep learning and medical diagnosis: A review of literature*, «Multimodal Technologies and Interaction», 2, 47, 1-12.
- CACCIARI I., POCOBELLI G.F. in press, *Machine Learning: A novel tool for archaeology*, in S. D'AMICO, V. VENUTI (eds.), *Handbook of Cultural Heritage Analysis*, Springer International Publishing.
- CACCIARI I., POCOBELLI G.F., CICOLA S., SIANO S. 2018, *Discrimination of soil texture and contour recognitions during archaeological excavation using Machine Learning*, «Institute of Physics Conference Series: Materials Science and Engineering», 364, 012042, 1-8.

- CACCIARI I., POCOBELLI G.F., SIANO S. 2017, *Machine Learning: A toolkit for speeding up archaeological stratigraphic identification*, in *3rd IMEKO International Conference on Metrology for Archaeology and Cultural Heritage. MetroArchaeo 2017 (Lecce 2017)*, 109-115 (<https://www.imeko.org/publications/tc4-Archaeo-2017/IMEKO-TC4-ARCHAEO-2017-023.pdf>).
- GU S., KELLY B., XIU D. 2020, *Empirical asset pricing via Machine Learning*, «The Review of Financial Studies», 33, 2223-2273.
- GUAITOLI M. (ed.) 2003, *Lo sguardo di Icaro. Le collezioni dell'Aerofototeca Nazionale per la conoscenza del territorio*, Catalogo della mostra, Roma, Campisano Editore.
- IBRAHEEM N.A., HASAN M.M., KHAN R.Z., MISHRA P.K. 2012, *Understanding color models: A review*, «ARPN Journal of Science and Technology», 2, 265-275.
- KAHU S.Y., RAUT R.B., BHURCHANDI K.M. 2019, *Review and evaluation of color spaces for image/video compression*, «Color Res Application», 44, 8-33.
- MEYER G.W., GREENBERG D.P. 1980, *Perceptual color spaces for computer graphics*, «Computer Graphics, ACM», 14, 254-261.
- MORETTI SGUBINI A.M., RICCIARDI L. 2011, *Considerazioni sulle testimonianze di Tuscania e di Vulci*, in *Tetti di terracotta. La decorazione architettonica fittile tra Etruria e Lazio in età arcaica. Atti delle Giornate di Studio (Roma 2010)*, Roma, Officina Edizioni, 75-86.
- MUSSON C., PALMER R., CAMPANA S. 2005, *In volo nel passato. Aerofotografia e cartografia archeologica*, Firenze, All'insegna del Giglio.
- OZDEMIR E., REMONDINO F. 2019, *Machine learning methods applied to WWII aerial images*, in *Geoprocessing and Archiving of Historical Aerial Images Workshop (Saint-Mandé, Paris 2019)* (http://www.eurosd.net/sites/default/files/images/inline/07_ozdemir_et al.pdf).
- PICCARRETA F. 1987, *Manuale di fotografia aerea. Uso archeologico*, Roma, L'Erma di Bretschneider.
- PICCARRETA F., CERAUDO G. 2000, *Manuale di aerofotografia archeologica. Metodologie, tecniche e applicazioni*, Bari, Edipuglia.
- POCOBELLI G.F. 2003, *Ortofotopiano storico del territorio di Vulci*, in GUAITOLI 2003, 147-156.
- POCOBELLI G.F. 2004, *Vulci: il contributo della fotografia aerea alla conoscenza dell'area urbana*, «Archeologia Aerea», 1, 127-143.
- POCOBELLI G.F. 2006, *La carta archeologica dell'area urbana di Vulci. Cartografia archeologica e fotogrammetria finalizzata*, Tesi di Dottorato in Topografia Antica (Università di Salerno, Roma La Sapienza, UniTuscia, UniSalento).
- POCOBELLI G.F. 2007, *Il territorio suburbano di Vulci attraverso le evidenze aerofotografiche. Viabilità e necropoli*, «Archeologia Aerea», 2, 167-185.
- POCOBELLI G.F. 2011, *Vulci e il suo territorio: area urbana, necropoli e viabilità. Applicazioni di cartografia archeologica e fotogrammetria finalizzata*, in G. CERAUDO (ed.), *100 anni di archeologia aerea in Italia. Atti del I Convegno Internazionale (Roma 2009)*, Foggia, Claudio Grenzi Editore, 117-126.
- PORTUGAL I., ALENCAR P., COWAN D. 2018, *The use of machine learning algorithms in recommender systems: A systematic review*, «Expert Systems with Applications», 97, 205-227.
- REILLY P., RAHTZ S. (eds.) 1992, *Archaeology and the Information Age: A Global Perspective*, London-New York, Routledge.
- SHEPHERD E.J., CERAUDO S., SALERNO G., REMONDINO F. 2019, *Analog/digital image processing of historical aerial imagery in the Italian National Photographic Aerial Archive (AFN-ICCD)*, in *Geoprocessing and Archiving of Historical Aerial Images Workshop (Saint-Mandé, Paris 2019)* (http://www.eurosd.net/sites/default/files/images/inline/04_shepherd_et al_italy.pdf).
- XU J., XUE K., ZHANG K. 2019, *Current status and future trends of clinical diagnoses via image-based deep learning*, «Theranostics», 9, 7556-7565.

ABSTRACT

On the basis of the research activity carried out as part of the Archeo 3.0 project 'Integration of key enabling technologies for the efficiency of preventive archaeological excavations', the authors explore the feasibility and limits of the automated approach for the recognition of archaeological marks. This approach is mainly motivated by the relevance that aerial photographs play in the reconstruction of ancient topography of human settlements. For this aim, a collection of historical aerial photographs of both the city and the necropolis of Vulci has been considered. These photographs, in colour and B/W, have been previously used in a PhD thesis in Ancient Topography in which the traditional methodology (photointerpretation and cartographic restitution) has been fully exploited. In this work, a systematic study is presented in order to compare the results obtained with Machine Learning techniques vs traditional ones. This comparison allows us to discuss the strengths and limits of both methodologies.